Chapter 2

Imaging MS Analysis in *Catharanthus roseus*

Kotaro Yamamoto, Katsutoshi Takahashi, Sarah E. O'Connor, and Tetsuro Mimura

Abstract

To understand how the plant regulates metabolism, it is important to determine where metabolites localize in the tissues and cells. Single-cell level omics approaches in plants have shown remarkable development over the last several years, and this data has been instrumental in gene discovery efforts for enzymes and transporters involved in metabolism. For metabolomics, Imaging Mass Spectrometry (IMS) is a powerful tool to map the spatial distribution of molecules in the tissue. Here, we describe the methods which we used to reveal where secondary metabolites, primarily alkaloids, localize in *Catharanthus roseus* stem and leaf tissues.

Key words Imaging MS, Single-cell metabolomics, Alkaloid, Specialized metabolism, Idioblast cell, Laticifer cell, *Catharanthus roseus*, Apocynaceae

1 Introduction

In multicellular organisms, a variety of cell types combine to form tissues and organs to maintain their vital activities. Although there are many unique cell types which perform different functions in the tissue, historically, life sciences drew conclusions from averaged data across entire tissues or organs. However, to understand living organisms precisely, unique cell types should also be investigated individually.

Recent technological developments now enable us to obtain information with high spatial resolution at the single-cell level. Next-generation and third-generation sequencing approaches have made it possible to generate single-cell gene expression profile datasets [1, 2]. Protein analysis remains challenging, since proteins cannot be amplified unlike DNA and RNA, but high-sensitivity MS analysis and separation technology have now been developed to obtain proteomics data from small numbers of cells [3, 4]. Simultaneously, metabolomic approaches using just a few cells have been

Vincent Courdavault and Sébastien Besseau (eds.), *Catharanthus roseus: Methods and Protocols*,
Methods in Molecular Biology, vol. 2505, https://doi.org/10.1007/978-1-0716-2349-7_2,

developed [5]. A key technique in single-cell mass spectrometry applications is Imaging Mass Spectrometry (IMS), which uses matrix-assisted laser desorption/ionization (MALDI) to visualize distribution of metabolites with high spatial resolution. Tissue samples are fixed, immobilized, and treated with a matrix. The metabolites within the tissue sample are ionized by laser irradiation, and then automatically injected to the mass spectrometer. This process is repeated iteratively across the tissue sample, at which point several tens or hundreds of thousands of mass spectrometric datasets are acquired. These datasets are then compiled into a reconstructed two-dimensional image based on the obtained MS data. IMS is now recognized as a robust method to understand the distribution of metabolites across a tissue section with high spatial resolution [5, 6].

Recently, single-cell omics approaches have been applied to plants. Plants pose several challenges in the application of these approaches, most notably a tough exterior cell wall that often requires protoplasting. However, IMS is well-suited for plant cell physiology, and applications of this method to a variety of plant systems have been reported [5].

Terpenoid indole alkaloids (TIAs) constitute one of the largest groups of alkaloids. TIAs, which contain over 3000 structurally distinct members, are observed in at least five plant families. Many TIAs have potent biological activities and pharmaceutical importance, for example, antitumor drugs such as vinblastine and vincristine [7]. *Catharanthus roseus* (L.) G. Don (Apocynaceae) is one of the best-characterized TIA-containing plants and produces more than 130 TIAs from strictosidine, the central precursor for all TIAs (Fig. 1a) [8, 9]. Interestingly, TIAs are produced in a variety of cell types in *C. roseus*. The current localization model has been deduced from the results of in situ RNA hybridization and immunocytochemical localization of TIA metabolic enzymes in leaf tissues. Strictosidine is derived from the secoiridoid, secologanin. The early stage of secoiridoid metabolism takes place in internal phloem-associated parenchyma cells (IPAP cells). The late-stage iridoid product, loganic acid, is then transported to epidermal cells [10, 11], where it is subsequently transformed into secologanin. Strictosidine, associated TIA intermediates, and other TIAs are also produced in the epidermal cells (Fig. 1) [10, 11]. Finally, a late-stage TIA intermediate, desacetoxyvindoline, is transported from epidermal cells to the idioblast cells or laticifer cells where it is accumulated in the vacuole [10–12].

Previously, our understanding of TIA metabolite localization was inferred from the localization of the transcripts or the correspond enzymes that carry out the biosynthesis of these metabolites. However, direct measurements of the metabolites within specific cell types were lacking. Therefore, we used state-of-the-art IMS, in conjugation with single-cell MS, to detect metabolites in situ at the

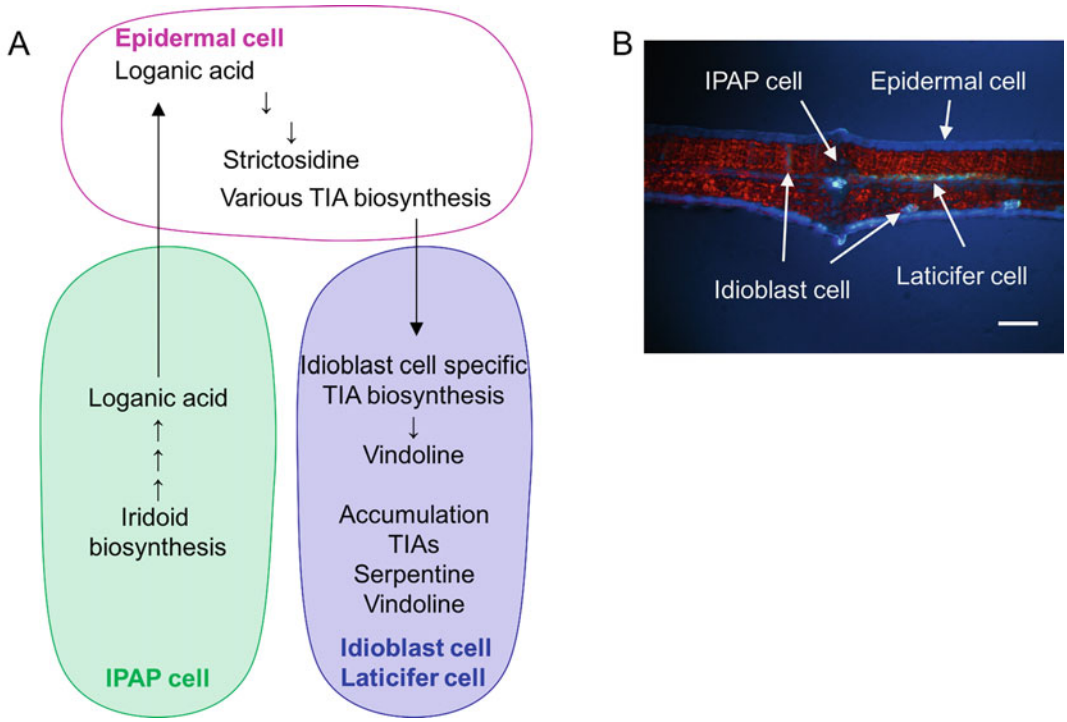

Fig. 1 TIA biosynthesis in *Catharanthus roseus*. (**a**) TIAs are produced in various distinct cell types in *Catharanthus roseus*. The early stage of secoiridoid metabolism takes place in internal phloem-associated parenchyma cells (IPAP cells). Then, loganic acid is transported to epidermal cells, where it is subsequently converted into strictosidine. Associated TIA intermediates and other TIAs are also produced in the epidermal cells. Finally, a late-stage TIA intermediate, desacetoxyvindoline, is transported from epidermal cells to the idioblast cells or laticifer cells, and late-stage TIAs are accumulated in the vacuoles of those cells. (**b**) A section of *C. roseus* leaf tissue excited with UV. Scale bar = 100 μm

cellular level in leaf and stem tissues of *C. roseus* [6, 13–16]. Here, we describe the sample preparation and method for IMS (Fig. 2).

2 Material

2.1 Plant Material

1. *C. roseus* (L.) G Don (cv. Equator White Eye) was germinated from seed (Sakata Seed Corporation, Yokohama, Japan) (*see* **Note 1**).

2.2 LC-MS Measurement

1. Stainless beads for 2 mL tube.
2. Multibeads shocker.
3. Liquid nitrogen.
4. Extraction solution: 0.5% formic acid and 1 ppm vindoline-d3 in methanol as an internal standard (*see* **Note 2**).
5. HPLC system coupled to a LTQ-Orbitrap.

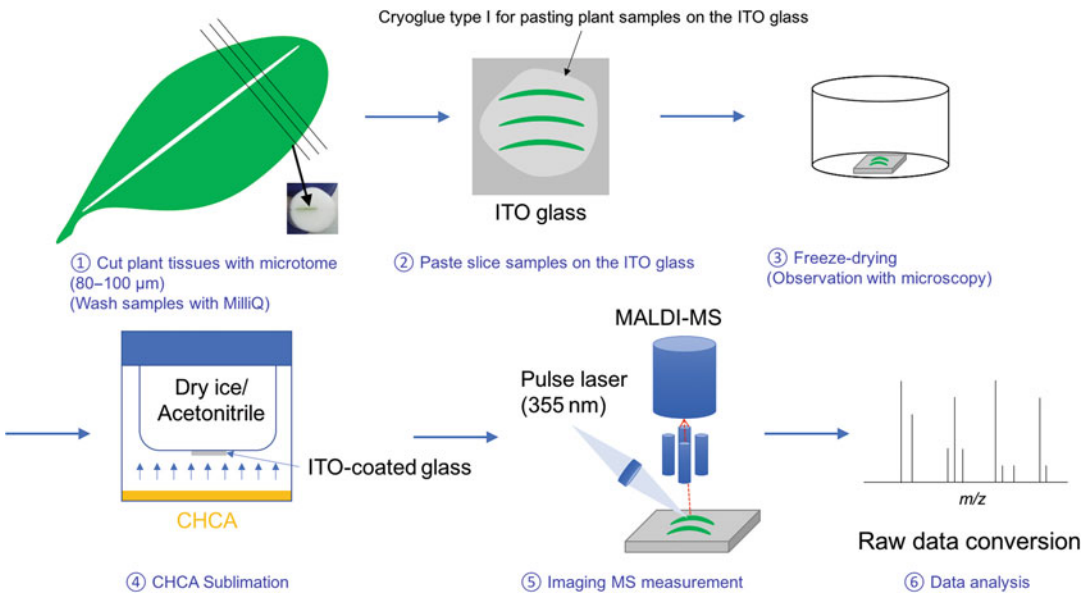

Fig. 2 Workflow for Imaging Mass Spectrometry (IMS) analysis

6. Reverse-phase C18 octadecylsilyl silica column (5 μm, 4.6 × 150 mm).
7. Solvent A: 25 mM ammonium acetate.
8. Solvent B: acetonitrile.

2.3 Equipment for Imaging MS

1. Microtome.
2. Indium tin oxide (ITO)-coated glass slide (11 mm × 11 mm × 0.7 mm).
3. Cryoglue type I.
4. Fluorescence stereomicroscope equipped with a ultraviolet long pass filter.
5. Freeze-dryer.
6. Alpha-cyano-4-hydroxycinnamic acid (CHCA).
7. 2,3-Dihydroxybenzoic acid (DHBA).
8. Sublimation apparatus (e.g., ChemGlass CG-3038, ChemGlass Life Sciences).
9. Heating plate.
10. Dry ice/acetonitrile.
11. Full solid-state UV-laser FTSS-355-Q4 (CryLas).
12. UV-laser focus optics.
13. A MALDI/LDI ion source was combined with a commercial FT-ICR mass spectrometer (APEX-Qe-9.4T with dual source; Bruker Daltonics Inc.) equipped with a 9.4 T superconductive magnet and video microscope (DZ3-E; Union optics).

2.4 Software

1. CompassXport software (Bruker Daltonics Inc.).
2. ProteoWizard msconverter [17].
3. mzml_to_imzml converter [18].
4. LabMSI in-house software [6], under the LabView environment (National Instruments).

3 Methods

3.1 LC-MS Analysis of Plant Tissue

1. Plant tissue (stem or leaf) was harvested from 1- to 3-month-old *C. roseus* for LC-MS and IMS measurements.
2. A portion of these samples (10–200 mg fresh weight) was frozen with liquid nitrogen immediately after harvesting and ground to fine powder by frost shattering with Multibeads shocker. Metabolomic data were generated for several tissues and developmental stages, with the identities of key selected alkaloids identified with reference standards.
3. Metabolites were extracted from the powdered sample with 1 mL extraction solution.
4. Samples were lyophilized by freeze drying and stored at −80 °C.
5. Samples were resuspended in 1-mL methanol immediately prior to measurement.
6. Tissue extracts (0.5–2 μL) were analyzed by LC-MS. The ratio of solvent A to B was isocratic at 20:80. TIAs were separated by reverse-phase octadecylsilyl silica column for 40 min. The flow rate was 0.25 mL/min at 40 °C. The spray voltage for positive measurement was 3800 V. Target mass peaks were detected in ± 5 ppm. We also conducted MS/MS analysis for each TIA peak for which a reference standard was available.

3.2 Preparation of Plant Tissues for Imaging MS

1. Plant tissue (stem or leaf) from 3.1 was washed with MilliQ water three times to remove the soil and dirt.
2. Then, plant tissue samples were embedded with a cylinder made of formed polystyrene.
3. Plant samples were cut into the slices of 80- to 100-μm thickness with the microtome (Fig. 2).
4. Those section samples were gently captured with flat tip tweezers to transfer to the petri dish. Those were washed with MilliQ water three times in the new petri dishes before transferring onto an indium tin oxide (ITO)-coated glass slide. Cryoglue type I was used to adhere the section onto the ITO-coated glass (*see* **Notes 3** and **4**).

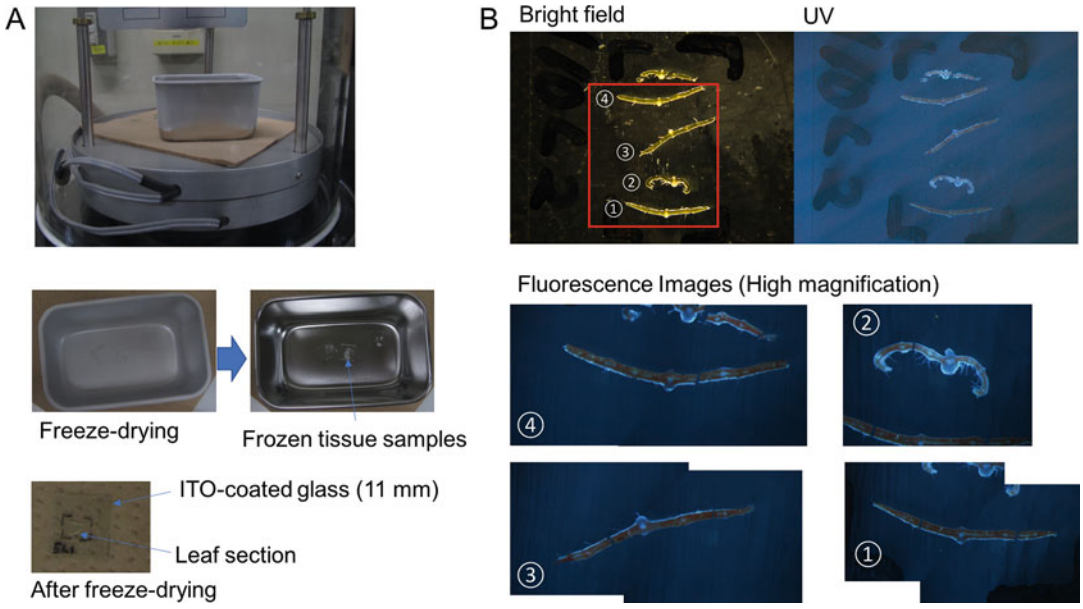

Fig. 3 Sample preparation of plant tissues sections. (**a**) Lyophilizing of leaf tissue samples in a freeze-dryer. (**b**) The leaf section samples after freeze-drying visualized by fluorescence microscopy

5. Plant tissue sections were examined under a fluorescence stereo microscope to check the integrity of the tissue and to determine which regions were suitable to use for IMS measurements (Fig. 1b).
6. The plant sections adhered to the ITO-coated glass slides were lyophilized with a freeze-dryer (Fig. 3) (*see* **Note 5**).
7. After lyophilization, the samples were again checked under the fluorescence stereo microscope for sample integrity. Samples were stored in tubes filled with nitrogen gas or under vacuum condition until IMS analysis.
8. Immediately prior to IMS, lyophilized plant samples were sublimated with CHCA (alpha-cyano-4-hydroxycinnamic acid) or DHBA (2,3-Dihydroxybenzoic acid). To accomplish this, freeze-dried samples were placed in the sublimation apparatus, and then the powder of CHCA or DHBA was added (Fig. 4c). The glassware of the sublimation apparatus was heated using a heating plate placed underneath the apparatus under vacuum. During the sublimation process, sample specimens were cooled using dry ice/hexane or dry ice/acetonitrile to condense the matrix vapor onto the sample specimen (Fig. 4c, d). DHBA was sublimated for 15 min at 150 °C, while CHCA was sublimated for 45 min at 230 °C.
9. After sublimation, a photo of the sample was taken for reference to compare with the IMS images to be generated.

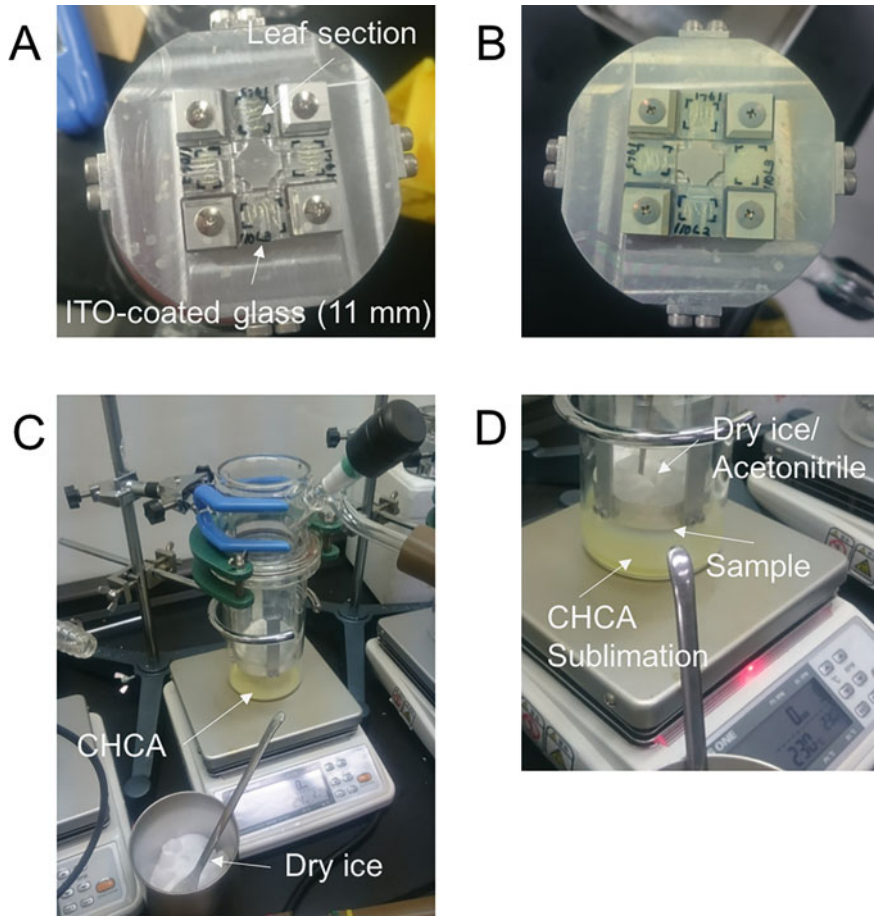

Fig. 4 The vapor deposition of CHCA on the ITO-coated glass. (**a**) Before vapor deposition. (**b**) After vapor deposition. (**c**) Sublimation apparatus with ITO-coated glass and CHCA. (**d**) CHCA sublimation on the ITO-coated glass

3.3 Imaging MS Measurement

1. The prepared plant sample on the ITO-coated glass slide was inserted horizontally into the ion-funnel cartridge.
2. The XYZ position was controlled with <1 μm precision.
3. A high-magnification and long-working distance video microscope was installed to view the sample specimen placed onto the ITO-coated glass slide from the bottom.
4. The position of the sample stage was controlled by a closed loop using software developed in-house using the LabView software development environment.
5. The specimen was ionized using a full solid-state UV-laser FTSS-355-Q4, which emits $\lambda = 355$ nm UV pulses of maximally 42 μJ pulse–1 with pulse length <1.4 ns at 1 kHz (*see* **Note 6**).

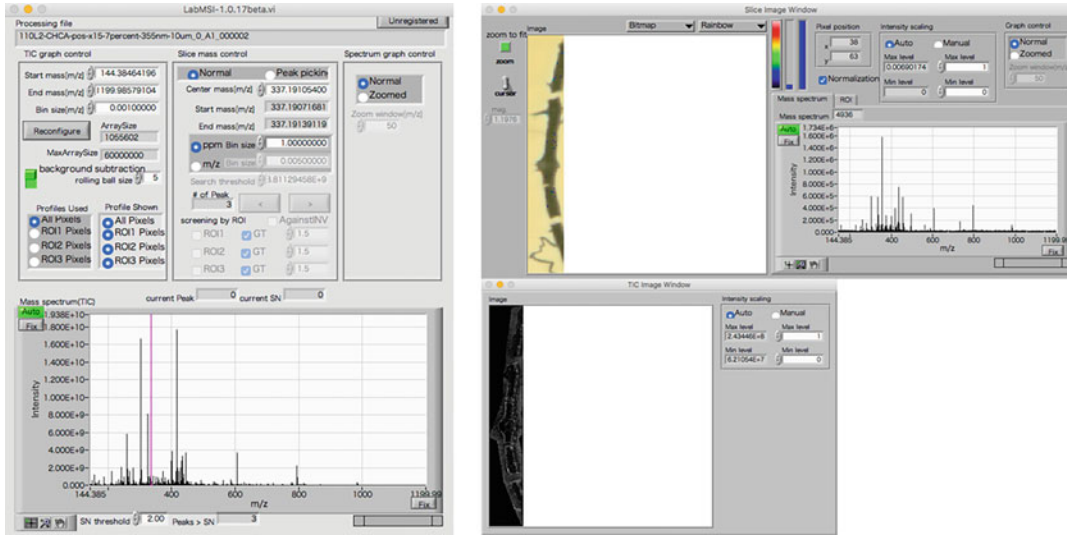

Fig. 5 Software and analysis with LabMSI. Screenshot from LabMSI-1.0.17 Software

6. The ions produced through the UV irradiation of the sample specimen surface were extracted and then ejected toward the ICR cell.
7. The time domain transient signal was transformed by fast Fourier transform (FFT) to give a frequency domain spectrum, and finally a high-resolution mass spectrum of the trapped ions was obtained (*see* **Note 7**).

3.4 Analysis of Metabolome Data

1. The series of mass spectrum data were stored in Bruker Daltonics's original raw format.
2. The raw data were then exported to mzML format using compassXport software and the ProteoWizard msconverter [17]. The mzML formatted file was then converted to imzML format [19] using the mzml_to_imzml converter [18], and the real position information of each pixel was embedded into the imzML file by in-house software (Figs. 5 and 6) [6].
3. An in-house software called "LabMSI" under the LabView environment was developed to process an average mass spectrum from among the whole pixels, to draw mass spectrum slice images of specific *m/z* values and to define the ROI (region of interest) to find ions which specifically belong to that area. LabMSI software shows three different windows, namely an average spectrum viewer, an MS slice viewer, and a TIC (total ion count) image viewer. On the average spectrum viewer, the mass spectrum averaged from all pixels can be displayed and an arbitrary slice of mass spectrum can be defined to draw an ion intensity image (MS slice image) on the MS slice viewer

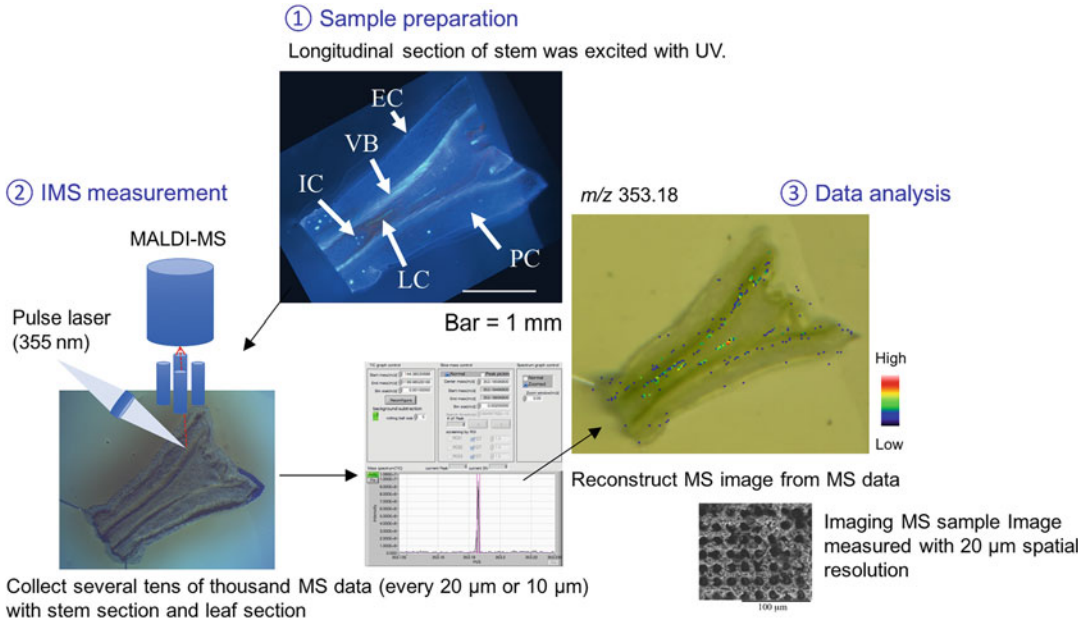

Fig. 6 IMS measurement and data analysis with LabMSI. Abbreviation in photos: EC: Epidermal cell, PC: Parenchyma cell, IC: Idioblast cell, LC: Laticifer cell, VB: Vascular bundle

window. The peaks on the average mass spectrum can be detected automatically, and the MS slice images corresponding to such selected peaks can be generated automatically. The central *m/z* value of the MS slice image (i.e., peak *m/z* value) is useful in determining the elemental composition of the corresponding ions, as this can also be used to make search queries to metabolite databases such as METLIN [20] or KNApSAcK [21].

4 Notes

1. *C. roseus* was grown at 25 °C under 14 light/10 dark h white fluorescent light photoperiod in a growth chamber.
2. We used vindoline-d3 as an internal standard for quantification of TIAs. Mass spectrometric detection was performed on LTQ-Orbitrap mounted on ESI ion source.
3. To distinguish cell types in mesophyll cells, we used serpentine as a visual marker. Serpentine is a TIA that localizes to idioblast cells and laticifer cells in *C. roseus*. When serpentine is excited with UV, this compound emits blue fluorescence around 445 nm [22] (Fig. 1b).
4. Before the section samples were adhered to the ITO-coated glass slide, we checked which sections contained laticifer cells

or idioblast cells by fluorescence stereomicroscopy. It was very difficult to pick the section which has every cell type. We used the youngest leaf tissue (around 1 cm long) for making leaf section samples, because we could most reliably observe laticifer cells in those leaves. In immature leaf tissue, it was easy to observe laticifer cell that accumulated serpentine under fluorescence microscopy.

5. Since samples could be crushed or melted during freeze-drying, keeping the position of alkaloids intact during this process was a concern. To avoid this, we put two to three drops of MilliQ water on the samples after we transferred section samples to the glass slide and placed the slide in a stainless steel box, and this box was floated on liquid nitrogen or dry ice/acetonitrile solution to freeze the samples. The stainless steel box containing the slide was transferred to the freeze-dryer before melting. This process greatly improved the integrity of the samples. We checked whether the freeze-dried section kept compounds in place by using the visual alkaloid marker, serpentine (Figs. 1b and 2).
6. Typically, 300 pulses of tightly focused UV laser ($\lambda = 355$ nm, pulse width = 1.4 ns, 7.0 μJ pulse−1 input for 1 kHz repetition laser) were applied to the surface of a matrix-coated or non-coated sample specimen surface to obtain a single mass spectrum.
7. The FTICR-mass spectrometer was calibrated using a d-arginine solution in 50% aqueous MeOH prior to the IMS run, and the mass spectrum was calibrated externally. The external calibration mass accuracy is expected to be approximately 1 ppm.

Acknowledgments

This work was supported by MEXT KAKENHI Grant Number JP22120006 and JSPS KAKENHI Grant Numbers JP24710235, JP18H05493, and Grant-in-Aid for JSPS Fellows 14J03616 and 20J00973. S.E.O. acknowledges ERC 788301.

References

1. Macosko EZ, Basu A, Satija R et al (2015) Highly parallel genome-wide expression profiling of individual cells using nanoliter droplets. Cell 161(5):1202–1214
2. Svensson V, Vento-Tormo R, Teichmann SA (2018) Exponential scaling of single-cell RNA-seq in the past decade. Nat Protoc 13: 599–604
3. Budnik B, Levy E, Harmange G et al (2018) SCoPE-MS: mass spectrometry of single mammalian cells quantifies proteome heterogeneity during cell differentiation. Genome Biol 19(1): 1–12
4. Marx V (2019) A dream of single-cell proteomics. Nat Methods 16:809–812

5. Dong Y, Li B, Aharoni A (2016) More than pictures: when MS imaging meets histology. Trends Plant Sci 21:686–698
6. Takahashi K, Kozuka T, Anegawa A et al (2015) Development and application of a high-resolution imaging mass spectrometer for the study of plant tissues. Plant Cell Physiol 56:1329–1338
7. Gigant B, Wang C, Ravelli RB et al (2005) Structural basis for the regulation of tubulin by vinblastine. Nature 435(7041):519–522
8. Van der Heijden R, Jacobs DI, Snoeijer W et al (2004) The Catharanthus alkaloids: pharmacognosy and biotechnology. Curr Med Chem 11:607–628
9. Verma P, Mathur AK, Srivastava A et al (2012) Emerging trends in research on spatial and temporal organization of terpenoid indole alkaloid pathway in Catharanthus roseus: a literature update. Protoplasma 249(2):255–268
10. Burlat V, Oudin A, Courtois M et al (2004) Co-expression of three MEP pathway genes and geraniol 10-hydroxylase in internal phloem parenchyma of Catharanthus roseus implicates multicellular translocation of intermediates during the biosynthesis of monoterpene indole alkaloids and isoprenoid-derived primary metabolites. Plant J 38(1):131–141
11. Ozber N, Watkins JL, Facchini PJ (2020) Back to the plant: overcoming roadblocks to the microbial production of pharmaceutically important plant natural products. J Ind Microbiol Biotechnol 47(9–10):815–828
12. Yoder LR, Mahlberg PG (1976) Reactions of alkaloid and histochemical indicators in laticifers and specialized parenchyma cells of Catharanthus roseus (Apocynaceae). Am J Bot 63(9):1167–1173
13. Mizuno H, Tsuyama N, Harada T et al (2008) Live single-cell video-mass spectrometry for cellular and subcellular molecular detection and cell classification. J Mass Spectrom 43: 1692–1700
14. Fujii T, Matsuda S, Tejedor ML et al (2015) Direct metabolomics for plant cells by live single-cell mass spectrometry. Nat Protoc 10(9):1445–1456
15. Yamamoto K, Takahashi K, Mizuno H et al (2016) Cell-specific localization of alkaloids in Catharanthus roseus stem tissue measured with imaging MS and single-cell MS. Proc Natl Acad Sci U S A 113:3891–3896
16. Yamamoto K, Takahashi K, Caputi L et al (2019) The complexity of intercellular localisation of alkaloids revealed by single-cell metabolomics. New Phytol 224:848–859
17. Kessner D, Chambers M, Burke R et al (2008) ProteoWizard: open source software for rapid proteomics tools development. Bioinformatics 24(21):2534–2536
18. Prince JT, Marcotte EM (2008) Mspire: mass spectrometry proteomics in Ruby. Bioinformatics 24(23):2796–2797
19. Schramm T, Hester Z, Klinkert I et al (2012) imzML--a common data format for the flexible exchange and processing of mass spectrometry imaging data. J Proteome 75(16):5106–5110
20. Smith CA, O'Maille G, Want EJ et al (2005) METLIN: a metabolite mass spectral database. Ther Drug Monit 27(6):747–751
21. Shinbo Y, Nakamura Y, Altaf-Ul-Amin M et al (2006) KNApSAcK: a comprehensive species-metabolite relationship database. In: Nagata T (ed) Biotechnology in agriculture and forestry. Plant metabolomics, vol 57. Springer, Berlin, Heidelberg, pp 165–181
22. Uzaki M, Yamamoto K, Murakami A et al (2022) Differential regulation of fluorescent alkaloid metabolism between idioblast and laticifer cells during leaf development in Catharanthus roseus seedlings. J Plant Res https://doi.org/10.1007/s10265-022-01380-1.